PHYSICS

Many-body thermodynamics on quantum computers via partition function zeros

Akhil Francis[1], Daiwei Zhu[2,3], Cinthia Huerta Alderete[2,4], Sonika Johri[5], Xiao Xiao[1], James K. Freericks[6], Christopher Monroe[2,3,5], Norbert M. Linke[2], Alexander F. Kemper[1]*

Partition functions are ubiquitous in physics: They are important in determining the thermodynamic properties of many-body systems and in understanding their phase transitions. As shown by Lee and Yang, analytically continuing the partition function to the complex plane allows us to obtain its zeros and thus the entire function. Moreover, the scaling and nature of these zeros can elucidate phase transitions. Here, we show how to find partition function zeros on noisy intermediate-scale trapped-ion quantum computers in a scalable manner, using the XXZ spin chain model as a prototype, and observe their transition from XY-like behavior to Ising-like behavior as a function of the anisotropy. While quantum computers cannot yet scale to the thermodynamic limit, our work provides a pathway to do so as hardware improves, allowing the future calculation of critical phenomena for systems beyond classical computing limits.

INTRODUCTION

Interacting quantum systems exhibit complex phenomena including phase transitions to various ordered phases. The universal nature of critical phenomena reduces their description to determining only the transition temperature and the critical exponents. However, numerically calculating these quantities for systems in new universality classes is complicated because of critical slowing down, requiring increasing resources near the critical point. An alternative approach is to analytically continue the calculation of the partition function to the complex plane and determine its zeros.

The partition function is a positive function of multiple real parameters representing physical quantities such as temperature and applied fields. When the partition function is analytically continued in one of the respective parameters, its zeros show notable structure for a variety of models of interest. Lee and Yang (1, 2) studied the partition function zeros of Ising-like systems in the complex plane of the magnetic field h and found that, at the critical temperature (and in the thermodynamic limit), the loci of zeros pinch to the real axis. Alternatively, Fisher (3) studied the partition function zeros by making the inverse temperature β complex.

Partition function zeros have been widely used (4, 5) in the analysis of thermodynamic phase transitions, dynamical phase transitions (6, 7), and critical exponents (8). The divergence of the free energy near the phase transition is intimately connected to the location of the partition function zero closest to the real axis (9, 10), and the critical scaling relations may be found from the density of zeros around a phase transition (11). Whenever the analytic continuation yields an analytic function in the complex plane (no poles or branch cuts), the partition function (and thus the free energy) can be reconstructed from the location of the zeros; this is typical because the partition function is a finite sum of exponentials for finite systems.

The complex values for the physical parameters typically have no real interpretation, limiting the partition function zeros principally to being useful mathematical constructs. They may be determined either exactly for solvable systems (5, 12, 13) (of which there are few) or through numerical methods (7, 14), which are limited by Hilbert space size in exact diagonalization or sampling issues in Monte Carlo methods. However, following work showing the use of an ancillary spin to probe quantum criticality (15, 16), Wei and Liu (17) observed that the mathematical structure arising from having complex physical parameters appears in the dynamics of quantum systems. They proposed an experiment to measure the zeros of the Ising model via the decoherence of a probe spin coupled to the Ising system; this was subsequently executed in a liquid of trimethyl phosphite molecules using nuclear magnetic resonance (18). While this beautifully demonstrates the technique, it is clearly not scalable, as it is difficult to design molecules for every envisioned situation.

Here, we use a probe spin—which within this context will be referred to as an ancilla qubit—to calculate the partition function zeros on a universal quantum computer, overcoming numerical difficulties in classical computation of quantum thermodynamics. In this manner, we can handle system sizes up to half the number of available qubits. We develop a quantum circuit that evolves a thermal state (19, 20) under an interaction with an ancilla qubit designed to represent the action of the complex field or temperature. Using this, we measure the zeros of the partition function of the XXZ spin chain model on a trapped-ion quantum computer and quantum circuit simulators as the model is tuned from Ising-like to XY-like. The locus of zeros undergoes clear qualitative changes, thus enabling the identification of a phase transition even on noisy intermediate-scale quantum (NISQ) hardware. With the design of the circuit being independent of a particular model, our approach goes beyond recent studies of the Ising model (21).

RESULTS

Partition function zeros

Our method applies to both Fisher and Lee-Yang zeros, which are zeros in the complex plane of inverse temperature β and a complex Hamiltonian field, respectively. First, we focus on the latter Lee-Yang

[1]Department of Physics, North Carolina State University, Raleigh, NC 27695, USA. [2]Joint Quantum Institute and Department of Physics, University of Maryland, College Park, MD 20742, USA. [3]Center for Quantum Information and Computer Science, University of Maryland, College Park, MD 20742, USA. [4]Instituto Nacional de Astrofísica, Óptica y Electrónica, Calle Luis Enrique Erro No. 1, Sta. Ma. Tonantzintla, Pue. CP 72840, Mexico. [5]IonQ Inc., 4505 Campus Dr, College Park, MD 20740, USA. [6]Department of Physics, Georgetown University, 37th and O Sts. NW, Washington, DC 20057, USA.
*Corresponding author. Email: akemper@ncsu.edu

case. We consider an arbitrary spin Hamiltonian $\mathcal{H}_s$ in the presence of an external magnetic field given by $\mathcal{H}_B = h \sum_i \sigma_i^z = h\mathcal{H}_I$. As in the original work by Lee and Yang (1), the external magnetic field is complex: $h = h_r + ih_i$. The partition function is then

$$\mathcal{Z}(\beta, h) = \text{Tr} \exp\left(-\beta\mathcal{H}_0 - i\beta h_i \sum_j \sigma_j^z\right) \quad (1)$$

where $\mathcal{H}_0 = \mathcal{H}_s + \text{Re}\,\mathcal{H}_{(B)}$. The system is initially prepared in a thermal state of $\mathcal{H}_0$ and then "time evolved" under $\mathcal{H}_I$ for a "duration" βh_i. This form suggests a direct measurement

$$L(h) = \frac{1}{\mathcal{Z}_0}\text{Tr} \exp\left(-\beta\mathcal{H}_0 - i\beta h_i \mathcal{H}_I\right) \equiv \frac{1}{\mathcal{Z}_0}\mathcal{Z}(\beta, h) \quad (2)$$

where $\mathcal{Z}_0 = \text{Tr}\, e^{-\beta\mathcal{H}_0} = \mathcal{Z}(\beta, h_r)$. The zeros of $L(h)$ are the Lee-Yang zeros of the partition function. For a finite system of N spins, we can reconstruct $\mathcal{Z}$ from its Lee-Yang zeros through the fundamental theorem of algebra, because the partition function is a polynomial in $\tilde{z} = \exp(2\beta h)$

$$\mathcal{Z}(\beta, \tilde{z}) = \mathcal{P}\prod_j (\tilde{z} - \tilde{z}_j) \quad (3)$$

where $\mathcal{P}$ is a numerical constant, independent of $\tilde{z}$.

As was discovered by Wei and Liu (17), $L(h)$ can be measured by coupling the system qubits to an ancilla qubit (or probe spin). Alternate proposals include measuring two-spin entanglement, but these have not yet been realized (22, 23). In the simplest case, when $\mathcal{H}_0$ and $\mathcal{H}_I$ commute, the necessary coupling Hamiltonian is given by

$$\mathcal{H}' = \frac{1}{2}(\sigma_{anc}^z \otimes \mathcal{H}_I) \quad (4)$$

with the evolution matrix $U(\beta h_i) = \exp(-i\beta h_i\mathcal{H}')$; for noncommuting Hamiltonians, a more complex $\mathcal{H}'$ must be constructed (24). With the ancilla initialized in a superposition state $|+\rangle$ and the system in its thermal state, the initial density matrix is

$$\rho(0) = (|+\rangle\langle+|) \otimes \frac{e^{-\beta\mathcal{H}_0}}{\mathcal{Z}_0} \quad (5)$$

After evolution with $U(\beta h_i)$ and tracing out the system qubits, the off-diagonal element of the ancilla density matrix is $L(h)$.

Fisher zeros are measured using an analogous procedure; since in this case β is complex, the evolution is with respect to the Hamiltonian $\mathcal{H}'$, where for Fisher zeros $\mathcal{H}_I = \mathcal{H}_0$, which always commutes with itself, and hence, Eq. (4) always applies. The evolution matrix for Fisher zeros is $U(\beta) = \exp(-i\beta\mathcal{H}')$.

Model

We apply the above method to the one-dimensional periodic XXZ spin chain model—an interacting spin model with anisotropy between spin exchange in the x-y plane versus spin exchange along the z direction—whose Hamiltonian is given by

$$\mathcal{H}_s = J\sum_i(\sigma_i^x\sigma_{i+1}^x + \sigma_i^y\sigma_{i+1}^y) + J_z\sum_i \sigma_i^z\sigma_{i+1}^z \quad (6)$$

We will work within the ferromagnetic Ising regime, i.e., $J_z = -|J_z|$. The model may be tuned between an Ising-like regime ($|J_z| \gg |J|$) and an XY-like regime ($|J_z| \ll |J|$) (see Fig. 1). To obtain the Lee-Yang zeros, we use a magnetic field $\mathcal{H}_B$ along the z axis.

The Lee-Yang zeros of the ferromagnetic Ising model are well known to be purely imaginary in h or to lie on the complex unit
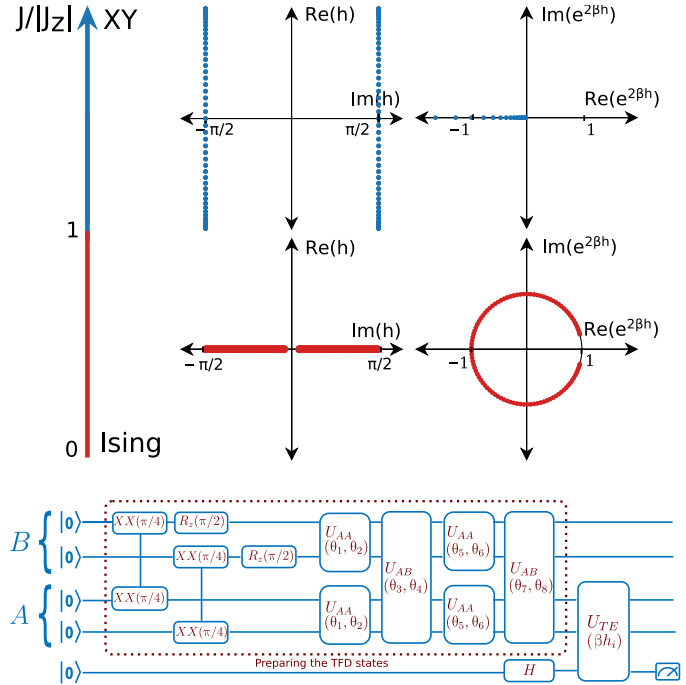

Fig. 1. Lee-Yang zeros for the limiting cases of the XXZ model and the quantum circuit for measuring them. (**Top**) Positions of the Lee-Yang zeros for 100-site Ising/XY models at $\beta = 1$ in the complex planes of h (left) and $\tilde{z} = e^{2\beta h}$ (right). For both Ising/XY models, the zeros in h occur away from the real axis. (**Bottom**) Circuit for obtaining partition function zeros. The TFD state is prepared using a variational quantum circuit. The thermal density matrix in subsystem A is subsequently evolved under a Hamiltonian coupling it to an ancilla spin. The ancilla coherence reflects the complex partition function. The measurement operation here represents the characterization of the real/imaginary parts of the coherences (off-diagonals) of the ancilla density matrix. We achieve this through measurement in both the x and y basis (see Materials and Methods for details).

circle in $\tilde{z} = \exp(2\beta h)$ (2, 17, 25). Figure 1 shows the position of the zeros in the complex planes of h and $\tilde{z}$ for a 100-site chain. At the other end, i.e., in the XY-like regime, the Lee-Yang zeros are qualitatively different. The zeros (in h) have a constant imaginary component $2\beta h_i = (2n + 1)\pi$, and their real part is given by the dispersion of the model after diagonalization via Jordan-Wigner transformation $h_r = -2J\cos(k)$ (5) (in the quantum circuit, any finite h_r must be included in the thermal state preparation). In between these limits, the zeros transition from one type to the other; we denote the character of the zeros as Ising-like or XY-like for the two cases, respectively. For zero temperature, the ground state abruptly changes from Ising-like to XY-like at $J = |J_z|$, but for finite temperatures, this becomes a gradual change.

Quantum circuit

The circuit is constructed in two parts. First, a thermal state corresponding to the XXZ spin chain model at finite temperature needs to be produced. For this, we prepare a thermofield double (TFD) state (19, 20), which is a purification of the thermal Gibbs state; it involves a doubling of the number of system qubits, half of which are then discarded to produce the thermal density matrix (see Fig. 1). Several methods to prepare TFD states exist (20, 26, 27). Here, we use a variational procedure reminiscent of the quantum approximate

optimization algorithm (QAOA) (28), consisting of the application of alternating Hamiltonians within and between the subsystems of the TFD state. The parameters (angles) are optimized classically (see the Supplementary Materials). Next, we perform evolution under the coupling Hamiltonian $\mathcal{H}_I$, which is straightforwardly implemented as controlled rotations on the ancilla qubit. Last, we measure the off-diagonal elements of the ancilla. For implementation on the trapped-ion hardware, U_{AA}, U_{AB}, and U_{TE} are broken down into native XX gates (see Materials and Methods and the Supplementary Materials), where the rotation angles in U_{AA} and U_{AB} are determined by the TFD optimization. To simulate an N site system, 2N + 1 qubits are required, where the factor of 2 comes from the doubling required for preparing the TFD state.

The general difficulties in preparing an arbitrary thermal state (29) cannot be avoided. For preparing TFD states, although empirically the number of QAOA steps scales linearly in the system size (19), the classical optimization is a costly step. A hybrid optimization is also possible based on a measurement of the Rényi entropy (30–34).

However, a number of alternate approaches to producing thermal states already exist; these include approaches where the thermal state is directly produced on a subset of the quantum hardware (35–41), and those where the sampling over the density matrix is performed classically (42, 43). Given a thermal state prepared by any of these methods, the partition function zeros are then obtained via a unitary evolution, which does not require any further scaling with the system size.

Implementation on trapped-ion hardware
Figure 2 shows the results on the two-site XXZ model, where we focus on the behavior of the zeros around the phase transition at $J \approx |J_z|$; we use β = 10 and $J_z = -1$. The figure shows the magnitude and real/imaginary parts of the ancilla coherence $L(h)$ in the top and bottom panels, respectively. The Lee-Yang zeros are found where both the real and imaginary parts of $L(h)$ vanish. When $J < |J_z|$, the zeros have no real part, in agreement with the general results for Ising-like zeros (see Fig. 1), and for two sites, we expect two zeros, symmetric about $\beta h_i = \pi/2$; these are shown in the top panel plots of $|L(h)|$. The bottom panels present the real and imaginary parts of $L(h)$ as a function of βh_i (a cut along constant h_r as indicated in the top panel), comparing the exact result and the experimental results

from the trapped-ion quantum computer. Although the exact position of the zeros is slightly different in the experiment, the qualitative behavior is clearly the same; $L(h)$ is entirely real, starts at unity, and changes sign once in between βh_i values of 0 and $\pi/2$. As J is increased toward the transition, the minimum in the real part of $L(h)$ gets shallow.

At the phase transition, the character of the zeros changes: βh_i becomes fixed at $\pi/2$, and the real part h_r becomes nonzero. We track h_r by including it in the TFD state preparation part of the circuit, and continue to sweep βh_i (indicated by horizontal lines in the top panels). This transition occurs in between $J/|J_z|$ values 1.03 and 1.06. On the XY-like side of the phase transition, the real part of $L(h)$ only touches zero at $\beta h_i = \pi/2$, and $L(h)$ acquires a nonzero imaginary part. This behavior is also captured correctly by the quantum computer; the experimental data are shown in the rightmost panel.

These data demonstrate that even with current generation NISQ hardware, a phase transition can be identified via the qualitative character of the Lee-Yang zeros and the ancilla coherence. This is an advantage of this method; rather than relying on a precise measurement of a quantity (such as the position of the zeros), a qualitative difference is sufficient to distinguish the Ising-like from the XY-like regime of the model. Understanding the effect of the noise in the quantum computer on the results can further help to predict the accuracy of the locations of the zeros as the system size grows larger (see the Supplementary Materials).

The experimental results also show that the zeros are robust to deviations of the prepared density matrix from the optimized result obtained from the variational TFD procedure. The implementation on the quantum computer inevitably introduces noise because of the inherent errors in the gates, resulting in $L(h)$ never being simultaneously zero in both real and imaginary components. These differences are consistent with errors in the experimental parameters, as shown in section SIII. Nevertheless, the qualitative patterns remain clear; furthermore, as we will show below, finding the smallest value of $|L(h)|$ by linear interpolation between the data points quantitatively identifies the correct location for the minimum.

Although here we have chosen to continue to sweep along βh_i and fix h_r, to avoid having to know an exact value of h_r, a sweep along constant h_i could also be performed. More generally, if nothing is
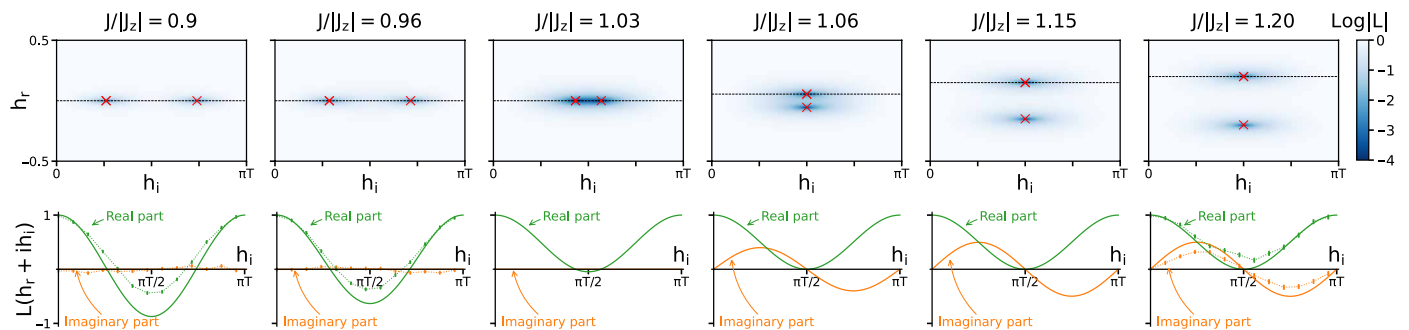

Fig. 2. Phase transition from Ising to XY at β=10 as demonstrated by the nature of the Lee-Yang zeros. (**Top**) False color plots of log $|L(h)|$ in complex h space. The line in the color plot shows the h values we are probing through the quantum circuit to find $L(h)$, where $h = h_r + ih_i$. The location of the zeros is marked in the top panels with a red cross. (**Bottom**) Real and imaginary parts of $L(h)$ along the cut indicated in the top row. Experimental results from the trapped-ion quantum computer are shown, with error bars connected with dotted lines. Around $J \approx |J_z|$, the nature of the zeros changes qualitatively from Ising-like to XY-like. The error bars on the experimental results correspond to the measurement statistical error.
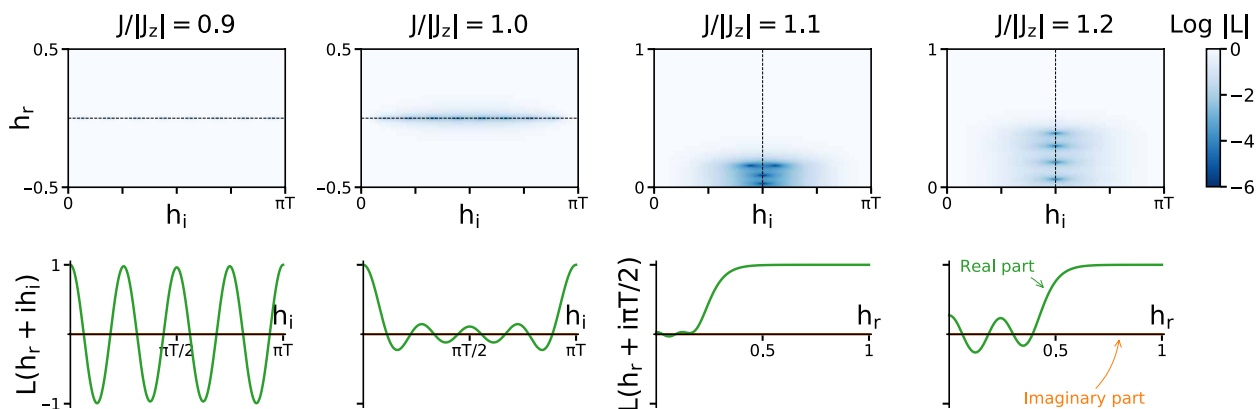
Fig. 3. Lee-Yang zeros for the eight-site XXZ model. (**Top**) The color plots show log $|L(h)|$ in complex h space. (**Bottom**) Cuts along the lines indicated in the corresponding top panel; note that for $J > |J_z|$, the cuts are vertical.
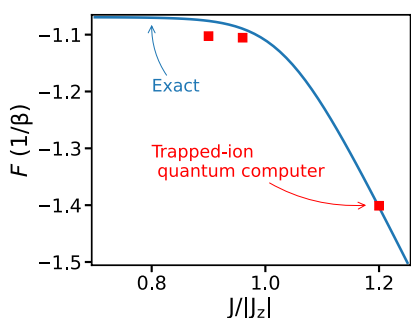

Fig. 4. Free energy of the two-site XXZ model at β=10 reconstructed from the Lee-Yang zeros. Red squares indicate F constructed using the experimental data. The experimental data were post-selected by discarding the states where the measured TFD qubits do not have the correct total magnetization (see the Supplementary Materials) before computing the free energy. The statistical error bars are smaller than the plot symbols.

known about the position of the zeros, then a full scan of complex h is possible by preparing a thermal state for each h_r. If a precise location of the individual zeros is required, then this will increase the computational effort; however, qualitative changes will remain clear. Moreover, knowledge of the first few zeros already yields thermodynamic information, as will be discussed below.

Our approach scales readily to larger systems. In Fig. 3, we show the results when the method is applied to an eight-site system. Because of hardware limitations (this calculation would require 17 qubits and a similarly larger number of gates for the TFD state preparation), only quantum circuit simulator data are available. The number of zeros is now larger, and they exhibit a more complex pattern, in particular around the phase transition. However, the overall qualitative difference between the two states remains clear—the zeros obtain a real part and shift to lie purely along the line $\beta h_i = \pi/2$.

DISCUSSION

Our results so far show that zeros of the partition function for a thermal state on a quantum computer may be obtained by the circuits shown in Fig. 1 (and Supplementary Materials), that these may be used to identify a phase transition by observing qualitative changes

in the nature of the zeros, and that this method can be executed on NISQ-era hardware. However, given the location of the zeros, we can reconstruct any thermodynamic quantity. As proof of principle, we focus on the free energy. While this is implicitly known in this case because a thermal state was prepared, this knowledge is not generally necessary. Although reconstructing the free energy involves the evaluation of an infinite sum, when a closed form can be obtained the full thermodynamics are determined. Here, this is accomplished by considering the polynomial in $\tilde{z} \equiv \exp(2\beta h_i)$ instead of h_i (this is because the energy spacing of the initial spin model is uniform). From the results shown in Fig. 2, we can extract the set of Lee-Yang zeros $\{h_0\}$, or equivalently $\{\tilde{z}_0\}$ once the prefactor $\mathcal{P}$ in the polynomial expansion is determined (see the Supplementary Materials). From the partition function, we compute the free energy at zero field $F = -(1/\beta) \ln \mathcal{Z}(\beta, h = 0)$, shown in Fig. 2. In the experimental data, $L(h)$ is never precisely zero; instead, we find the value of h_i corresponding to the smallest value of $|L(h)|$ by linear interpolation between the data points (h_r is assumed to be known from the TFD preparation). The reconstructed free energy is shown in Fig. 4, where we have used data that were post-selected to have the correct total magnetization; the agreement between the exact values and those obtained from the trapped-ion quantum computer is very good.

Beyond exactly reconstructing the partition function, the zeros also yield information regarding the thermodynamic properties near the phase transition. The partition function zeros lead to divergences in the free energy; moreover, in the limit $N \to \infty$, the zeros form a branch cut ending in an edge singularity. It is known from complex analysis that the knowledge of a function around its branch cuts is sufficient to determine the entire function. Furthermore, even if only the first zero is known (i.e., the closest zero to the positive real axis of $\tilde{z}$ or the edge singularity), then the temperature and field dependence of thermodynamic functions is dominated by its position (9, 10): In the expansion of a complex function near a singularity, the terms after some order n are determined by the properties of the singularity. Last, Abe (11) showed that the dependence of density of zeros on the system size (i.e., finite size scaling) can be used to determine critical exponents of the phase transition. The limiting density of zeros may also be used to characterize the phase transition (44).

Hence, studying partition function zeros on a quantum computer can efficiently determine much of the critical phenomena at

the transition. A similar approach has been used to study distributions of many-body observables in spin systems using quantum computers (45).

In this work, we have outlined how partition function zeros may be obtained and demonstrated that this is feasible even on NISQ hardware. Thus, as improvements to quantum computers enable ever growing complex calculations, partition function zeros can play a broadly applicable role in the simulation of physics at zero and finite temperatures. They may be evaluated with relative ease with a suitably chosen time evolution and yield a wealth of information regarding the thermodynamics of the system under study.

MATERIALS AND METHODS

We use a reconfigurable digital quantum computer for this study. The system is made of a chain of $^{171}Yb^+$ ions trapped with a radio frequency electric field (46). The qubits are made of a pair of states in the hyperfine-split $^2S_{1/2}$ ground-level manifold of each ion, connected by a magnetic field–insensitive 12.642821-GHz transition. We use optical pumping to initialize qubits to $|0\rangle$. The qubit readout is implemented via the state-dependent fluorescence detection (47). The complete set of quantum gates is realized with a pair of Raman beams derived from a single 355-nm mode-locked laser. Our native single-qubit gates are rotations along arbitrary axes in the XY plane of the Bloch sphere by arbitrary angles, achieved by driving resonant Raman transitions of defined phases. Our native two-qubit gates are XX (Ising) gate based on the phonon-mediated Molmer-Sorensen interaction (48, 49). Our scheme uses multiple phonon modes to reach optimal performance. An amplitude modulation technique is applied to disentangle the phonon modes from the qubits at the end of each two-qubit gate (50). Our single- and two-qubit gate fidelities are typically around 99.5(2)% and 98 to 99%, respectively. The residual entanglement between the qubits and the phonon modes is the primary factor limiting the fidelity of each two-qubit gate. In addition, for circuits used in this study, which involve 20 two-qubit gates, heating of phonon modes also plays a nontrivial role.

The qubit readout is simultaneously performed on all the qubits in the computational (Z) basis. We append the circuit with an additional $R_y(-\pi/2)$ or $R_x(\pi/2)$ rotation to perform measurements in the X or Y basis, respectively. We repeated each circuit 2000 times to obtain the statistics of the observables, assuming that the outcomes follow the binomial distribution. The data have been corrected for readout error (dominantly cross-talk, ~1%) assuming perfect qubit initialization (initialization errors are measured to be <0.1%).

SUPPLEMENTARY MATERIALS

Supplementary material for this article is available at http://advances.sciencemag.org/cgi/content/full/7/34/eabf2447/DC1

REFERENCES AND NOTES

1. C. N. Yang, T. D. Lee, Statistical theory of equations of state and phase transitions. I. Theory of condensation. *Phys. Rev.* **87**, 404–409 (1952).
2. T. D. Lee, C. N. Yang, Statistical theory of equations of state and phase transitions. II. Lattice gas and ising model. *Phys. Rev.* **87**, 410–419 (1952).
3. M. E. Fisher, *Lectures in Theoretical Physics*, Vol. VU C (University of Colorado Press, 1965).
4. M. Suzuki, M. E. Fisher, Zeros of the partition function for the Heisenberg, ferroelectric, and general Ising models. *J. Math. Phys.* **12**, 235–246 (1971).
5. P. Tong, X. Liu, Lee-Yang zeros of periodic and quasiperiodic anisotropic *XY* chains in a transverse field. *Phys. Rev. Lett.* **97**, 017201 (2006).
6. M. Heyl, A. Polkovnikov, S. Kehrein, Dynamical quantum phase transitions in the transverse-field Ising model. *Phys. Rev. Lett.* **110**, 135704 (2013).
7. K. Brandner, V. F. Maisi, J. P. Pekola, J. P. Garrahan, C. Flindt, Experimental determination of dynamical Lee-Yang zeros. *Phys. Rev. Lett.* **118**, 180601 (2017).
8. A. Deger, C. Flindt, Determination of universal critical exponents using Lee-Yang theory. *Phys. Rev. Res.* **1**, 023004 (2019).
9. G. Darboux, Mémoire sur l'approximation des fonctions de très-grands nombres, et sur une classe étendue de développements en série. *J. Math. Pure. Appl.* 5–56 (1878).
10. C. Hunter, B. Guerrieri, Deducing the properties of singularities of functions from their Taylor series coefficients. *SIAM J. Appl. Math.* **39**, 248–263 (1980).
11. R. Abe, Logarithmic singularity of specific heat near the transition point in the Ising model. *Prog. Theor. Phys.* **37**, 1070–1079 (1967).
12. G. L. Jones, Complex temperatures and phase transitions. *J. Math. Phys.* **7**, 2000–2005 (1966).
13. A. Connelly, G. Johnson, F. Rennecke, V. Skokov, Universal location of the Yang-Lee edge singularity in **O**(*N*) theories. *Phys. Rev. Lett.* **125**, 191602 (2020).
14. A. Deger, C. Flindt, Lee-Yang theory of the Curie-Weiss model and its rare fluctuations. *Phys. Rev. Res.* **2**, 033009 (2020).
15. H. T. Quan, Z. Song, X. F. Liu, P. Zanardi, C. P. Sun, Decay of Loschmidt echo enhanced by quantum criticality. *Phys. Rev. Lett.* **96**, 140604 (2006).
16. J. Zhang, X. Peng, N. Rajendran, D. Suter, Detection of quantum critical points by a probe qubit. *Phys. Rev. Lett.* **100**, 100501 (2008).
17. B. B. Wei, R. B. Liu, Lee-Yang zeros and critical times in decoherence of a probe spin coupled to a bath. *Phys. Rev. Lett.* **109**, 185701 (2012).
18. X. Peng, H. Zhou, B.-B. Wei, J. Cui, J. Du, R.-B. Liu, Experimental observation of Lee-Yang zeros. *Phys. Rev. Lett.* **114**, 010601 (2015).
19. J. Wu, T. H. Hsieh, Variational thermal quantum simulation via thermofield double states. *Phys. Rev. Lett.* **123**, 220502 (2019).
20. D. Zhu, S. Johri, N. M. Linke, K. A. Landsman, C. H. Alderete, N. H. Nguyen, A. Y. Matsuura, T. H. Hsieh, C. Monroe, Generation of thermofield double states and critical ground states with a quantum computer. *Proc. Natl. Acad. Sci. U.S.A.* **117**, 25402–25406 (2020).
21. A. Krishnan, M. Schmitt, R. Moessner, M. Heyl, Measuring complex-partition-function zeros of Ising models in quantum simulators. *Phys. Rev. A* **100**, 022125 (2019).
22. K. P. Gnatenko, A. Kargol, V. M. Tkachuk, Two-time correlation functions and the Lee-Yang zeros for an interacting Bose gas. *Phys. Rev. E* **96**, 032116 (2017).
23. A. R. Kuzmak, V. M. Tkachuk, Probing the Lee–Yang zeros of a spin bath by correlation functions and entanglement of two spins. *J. Phys. B At. Mol. Opt. Phys.* **52**, 205501 (2019).
24. B.-B. Wei, S.-W. Chen, H.-C. Po, R.-B. Liu, Phase transitions in the complex plane of physical parameters. *Sci. Rep.* **4**, 5202 (2014).
25. B.-B. Wei, Probing Yang–Lee edge singularity by central spin decoherence. *New J. Phys.* **19**, 083009 (2017).
26. W. Cottrell, B. Freivogel, D. M. Hofman, S. F. Lokhande, How to build the thermofield double state. *J. Energy Phys.* **2019**, 58 (2019).
27. J. Martyn, B. Swingle, Product spectrum ansatz and the simplicity of thermal states. *Phys. Rev. A* **100**, 032107 (2019).
28. E. Farhi, J. Goldstone, S. Gutmann, A quantum approximate optimization algorithm. arXiv:1411.4028 [quant-ph] (14 November 2014).
29. J. Kempe, A. Kitaev, O. Regev, The complexity of the local Hamiltonian problem. *SIAM J. Comput.* **35**, 1070–1097 (2006).
30. S. Johri, R. N. Bhatt, Singular behavior of eigenstates in Anderson's model of localization. *Phys. Rev. Lett.* **109**, 076402 (2012).
31. A. Misra, U. Singh, M. N. Bera, A. K. Rajagopal, Quantum Rényi relative entropies affirm universality of thermodynamics. *Phys. Rev. E* **92**, 042161 (2015).
32. S. Johri, D. S. Steiger, M. Troyer, Entanglement spectroscopy on a quantum computer. *Phys. Rev. B* **96**, 195136 (2017).
33. N. M. Linke, S. Johri, C. Figgatt, K. A. Landsman, A. Y. Matsuura, C. Monroe, Measuring the Rényi entropy of a two-site Fermi-Hubbard model on a trapped ion quantum computer. *Phys. Rev. A* **98**, 052334 (2018).
34. T. Brydges, A. Elben, P. Jurcevic, B. Vermersch, C. Maier, B. P. Lanyon, P. Zoller, R. Blatt, C. F. Roos, Probing Rényi entanglement entropy via randomized measurements. *Science* **364**, 260–263 (2019).
35. D. Poulin, P. Wocjan, Sampling from the thermal quantum Gibbs state and evaluating partition functions with a quantum computer. *Phys. Rev. Lett.* **103**, 220502 (2009).
36. A. Gilyén, "Quantum singular value transformation & its algorithmic applications," ILLC Dissertation Series (2019).
37. M. Motta, C. Sun, A. T. K. Tan, M. J. O'Rourke, E. Ye, A. J. Minnich, F. G. S. L. Brandão, G. K.-L. Chan, Determining eigenstates and thermal states on a quantum computer using quantum imaginary time evolution. *Nat. Phys.* **16**, 205–210 (2020).
38. M. Metcalf, J. E. Moussa, W. A. de Jong, M. Sarovar, Engineered thermalization and cooling of quantum many-body systems. *Phys. Rev. Res.* **2**, 023214 (2020).
39. S. Polla, Y. Herasymenko, T. E. O'Brien, Quantum digital cooling. arXiv:1909.10538 [quant-ph] (23 September 2019).
40. D.-B. Zhang, G.-Q. Zhang, Z.-Y. Xue, S.-L. Zhu, Z.. D. Wang, Continuous-variable assisted thermal quantum simulation. *Phys. Rev. Lett.* **127**, 020502 (2020).

41. M. Metcalf, E. Stone, K. Klymko, A. F. Kemper, M. Sarovar, W. A. de Jong, Quantum Markov chain Monte Carlo with digital dissipative dynamics on quantum computers. arXiv:2103.03207 [quant-ph] (4 March 2021).

42. S. R. White, Minimally entangled typical quantum states at finite temperature. *Phys. Rev. Lett.* **102**, 190601 (2009).

43. G. Verdon, J. Marks, S. Nanda, S. Leichenauer, J. Hidary, Quantum Hamiltonian-based models and the variational quantum thermalizer algorithm. arXiv:1910.02071 [quant-ph] (4 October 2019).

44. S. Grossmann, W. Rosenhauer, Temperature dependence near phase transitions in classical and quant. mech. canonical statistics. *Z. Phys.* **207**, 138–152 (1967).

45. Z. Xu, A. del Campo, Probing the full distribution of many-body observables by single-qubit interferometry. *Phys. Rev. Lett.* **122**, 160602 (2019).

46. S. Debnath, N. M. Linke, C. Figgatt, K. A. Landsman, K. Wright, C. Monroe, Demonstration of a small programmable quantum computer with atomic qubits. *Nature* **536**, 63–66 (2016).

47. S. Olmschenk, K. C. Younge, D. L. Moehring, D. N. Matsukevich, P. Maunz, C. Monroe, Manipulation and detection of a trapped Yb^+ hyperfine qubit. *Phys. Rev. A* **76**, 052314 (2007).

48. K. Mølmer, A. Sørensen, Multiparticle entanglement of hot trapped ions. *Phys. Rev. Lett.* **82**, 1835–1838 (1999).

49. E. Solano, R. L. de Matos Filho, N. Zagury, Deterministic Bell states and measurement of the motional state of two trapped ions. *Phys. Rev. A* **59**, R2539–R2543 (1999).

50. T. Choi, S. Debnath, T. A. Manning, C. Figgatt, Z.-X. Gong, L.-M. Duan, C. Monroe, Optimal quantum control of multimode couplings between trapped ion qubits for scalable entanglement. *Phys. Rev. Lett.* **112**, 190502 (2014).

51. G. Aleksandrowicz, T. Alexander, P. Barkoutsos, L. Bello, Y. Ben-Haim, D. Bucher, F. Jose Cabrera-Hernández, J. Carballo-Franquis, A. Chen, C.-F. Chen, J. M. Chow, A. D. Córcoles-Gonzales, A. J. Cross, A. Cross, J. Cruz-Benito, C. Culver, S. De La Puente González, E. De La Torre, D. Ding, E. Dumitrescu, I. Duran, P. Eendebak, M. Everitt, I. F. Sertage, A. Frisch, A. Fuhrer, J. Gambetta, B. G. Gago, J. Gomez-Mosquera, D. Greenberg, I. Hamamura, V. Havlicek, J. Hellmers, Ł. Herok, H. Horii, S. Hu, T. Imamichi, T. Itoko, A. Javadi-Abhari, N. Kanazawa, A. Karazeev, K. Krsulich, P. Liu, Y. Luh, Y. Maeng, M. Marques, F. Jose Martín-Fernández, Douglas T. McClure, D. M. Kay, S. Meesala, A. Mezzacapo, N. Moll, D. M. Rodríguez, G. Nannicini, P. Nation, P. Ollitrault, L. J. O'Riordan, H. Paik, J. Pérez, A. Phan, M. Pistoia, V. Prutyanov, M. Reuter, J. Rice, A. R. Davila, R. H. P. Rudy, M. Ryu, N. Sathaye, C. Schnabel, E. Schoute, K. Setia, Y. Shi, A. Silva, Y. Siraichi, S. Sivarajah, J. A. Smolin, M. Soeken, H. Takahashi, I. Tavernelli, C. Taylor, P. Taylour, K. Trabing, M. Treinish, W. Turner, D. Vogt-Lee, C. Vuillot, J. A. Wildstrom, J. Wilson, E. Winston, C. Wood, S. Wood, S. Wörner, I. Y. Akhalwaya, C. Zoufal, Qiskit: An open-source framework for quantum computing (2019); doi:10.5281/zenodo.2562110.

Citation: A. Francis, D. Zhu, C. Huerta Alderete, S. Johri, X. Xiao, J. K. Freericks, C. Monroe, N. M. Linke, A. F. Kemper, Many-body thermodynamics on quantum computers via partition function zeros. *Sci. Adv.* **7**, eabf2447 (2021).